



ACOUSTIC SIGNATURE OF FOUR CUTTERS EV BURNER USING PILOT INJECTOR FUEL SHIFT

Mustafa Osama

Mechanical Power Engineering Department
Faculty of Engineering-Mataria – Helwan
University, Cairo-Egypt

H. S. Ayoub

Physics Department
Faculty of Science, University of Cairo
Cairo, Egypt

Ahmed Emara

Mechanical Power Engineering Department
Faculty of Engineering-Mataria – Helwan
University, Cairo-Egypt

Adel Hussein

Mechanical Power Engineering Department
Faculty of Engineering-Mataria – Helwan
University, Cairo-Egypt

Hany Moneib

Mechanical Power Engineering Department
Faculty of Engineering-Mataria – Helwan
University, Cairo-Egypt

Ashraf F. El-Sherif

Engineering Physics Department
Military Technical College
Cairo, Egypt

ABSTRACT

The basic mechanisms leading to combustion oscillations is in the presence of pressure waves, the flow features large scale motions which drive the instability. The dynamics of the flame is then dominated by processes of hydrodynamic instability, vortex roll-up, vortex interactions, front and reacting stream pulsations, periodic extinctions and reignitions, self-acceleration.

Combustion instabilities are a major problem in the design of high performance propulsion systems (rocket motors, jet engine afterburners, ramjets). Instabilities are also observed in power plants and in various industrial processes. They are characterized by large oscillations of the flow parameters, which have many undesirable effects. Low frequency oscillations induce large mechanical vibrations in the system, including the combustion chamber, the feeding lines and the connected rotating machinery. Unstable operation enhances, the heat transfer rates at the combustor walls and in extreme cases this may lead to serious damage and even a total loss of the system.

The present work investigates the changes induced by pilot injections in the acoustic signature of a newly designed 4-slot EV burner using pilot injector at reacting and non-reacting conditions. These changes are affecting the flame stabilization especially in the lean premixed combustion due to the large structures resulting from vortex breakdown and the swirling shear-layers. Pilot injector offered good results in flame stability. The injector position influences the flow field and in turns the flame stability. Different pilot injector fuel shift inside the burner are tested.

All the results are to be compared with those obtained by the

previously developed 2-slot and 4-slot configuration without pilot injector. This allows the identification of the merits and/or drawbacks of both designs.

KEY WORDS

EV Gaseous Burner, Turbulent Flame,

INTRODUCTION

Gas turbine manufacturers have developed and continued to enhance lean premixed combustion systems to comply with emissions regulations for NO_x, carbon monoxides, and unburned hydrocarbons. Most of gas turbine injectors make swirl configurations that produce a central toroidal recirculation zones to provide the dominant flame stabilization mechanism (Yang 2005). Swirl increases fuel-air mixing, improves flame stabilization, and has a strong influence on flame characteristics and pollutant emissions (Emara 2009). The use of swirl to stabilize the reaction is taken of design practice from combustors designed to operate stoichiometrically. As such, the central recirculation zone provides a low velocity region that allows the reaction to anchor. Such strong swirl also causes high strain on the reaction.

The demand for gas turbine engines with reduced emission levels, stable combustion conditions and low specific fuel consumption is the goal at the past two decades (Rankin 2007). Combination of prior requirements is the way to an efficient combustion (Seyfried 2007). Strategies for reducing NO_x emissions from engines have been developed over these decades to comply with environmental concerns and government regulations. For power generation,



premixed gas turbine combustors need to be operated as lean as possible to secure sub-10 ppm concentrations of NO_x emission. In a combustor under fuel-lean conditions, achieving stable combustion requires overcoming several inter-related problems such as flame stabilization, flame stability and extinction, and combustion oscillations or thermoacoustic instabilities which depend on the boundary conditions of the engine.

Thermoacoustic instabilities can arise if pressure amplitude oscillations $p'(t)$ are in phase with heat release fluctuations $Q'(t)$ and if the acoustic energy E exceeds the dissipation losses.

Some significant stability and noise control breakthroughs have been developed by the gas turbine designers but it still in instability ranges and produces significant noise levels that must be mitigated or reduced to make these engines compatible with either environmental or occupational regulatory noise requirements (Giampaolo 2003). To suppress combustion oscillations some modifications are taken in consideration. These modifications are constriction of duct, use of resonators, use of sound absorbent material, modified sudden expansion, modified disk-type flame holder and modified fuelling arrangement.

It is common to rely on a pilot injector to operate lean premixed gas turbines. The pilot fuel allows the reaction to continue even if the reaction produced by the main fuel/air mixture starts to suffer some degree of instability. The pilot is generally directed into a strategic location in the combustor to enrich a region that will help sustain the reaction. A common location is along the centerline into a recirculation zone (Rankin 2007). Numerous experimental works have been performed to control or characterize combustion instabilities on the swirl stabilized burner (Albrecht 2008, Lacarelle 2008, and Paschereit 1999). Different pilot fuel injection types and locations have been tested and showed for several configurations positive results regarding NO_x and stability. An axisymmetric mode matching the $\frac{1}{4}$ wave of the resonance tube was typically occurring and dominated the instability mechanism. Phase averaged flame visualization showed that the flame is oscillating between two positions; one located inside the burner and the other located at the outlet of the burner. The oscillation of the flame position leads to an oscillation of the flame surface at the fuel injection location, generating fuel air ratio oscillations. Fuel air ratio fluctuations lead to oscillation of the heat release, which feeds the thermoacoustic cycle and may sustain combustion instabilities.

Albrecht is stabilizing the flame by a pilot fuel injection only. When switching on the pilot fuel, the flame stabilizes in numerous cases inside the burner, leading the diffusion like flame. This flame, when it is stable, has the disadvantage to generate high NO_x emissions. To circumvent this problem, Albrecht proposed to use premixed pilot fuel injection as well as pulsated pilot fuel injection

and decreased successfully the NO_x penalties compared to a standard pilot injection (Albrecht 2008). Lean burn combustors comprising round sudden expansions use a pilot stream at the core to stabilize an otherwise lean flow (Rankin 2007).

The present part of thesis work investigates the changes induced by pilot injections in the main flow field at reacting and non-reacting conditions in a swirl stabilized burner. The behavior of these injections, regarding stability and NO_x and CO emissions in that burner, is studied also at several acoustic boundary conditions represented in the combustion chamber length (short and long). These changes are affecting the flame stability especially in the lean premixed combustion due to large structures resulting from the vortex breakdown and the swirling shear-layers.

The Burner EV10 Four cutters

Description the EV-10 four cutters swirl stabilized burner FIG1 shows the premix burner with the additional burner ring surrounding the swirler arrangement, the premix burner 10 of FIG. 1 extends along a central burner axis 11. It comprises four identical shells 12 a-d, which are parts of a virtual cone, which opens into the downstream direction the shells are displaced from their original position in said virtual cone perpendicular to the burner axis to define a tangential slot 14 between each pair of adjacent shells. Through these slots 14 air enters into the interior of the conical shell arrangement in a swirling fashion. At each slot 14, a premix gas channel 13a-d, which runs along an axial edge of an adjacent shell, is provided to inject a gaseous fuel through holes fig 2 into the entering air stream. Now, the burner shells 12 a-d are extended and intersected

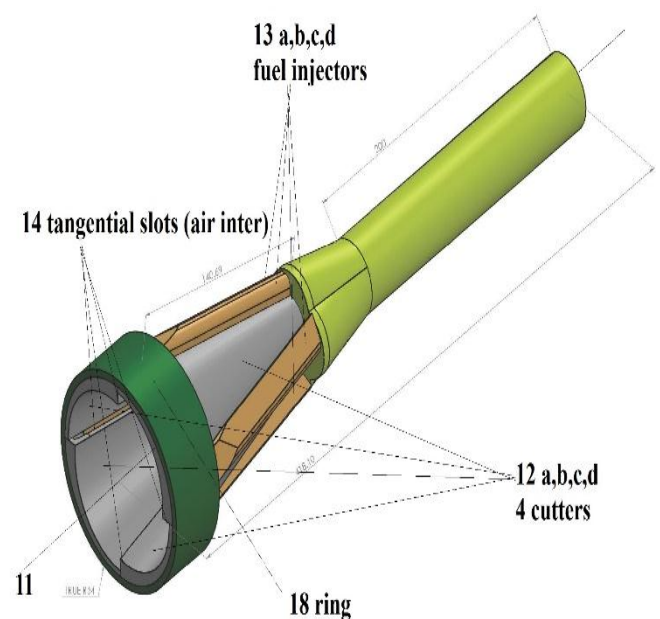


Fig 1 EV 10 4 cutters



Naturally with a virtual coaxial cylinder with a predetermined Radius R (shown FIG. 2), Which is adapted to the cylindrical shape of the subsequent mixing tube, thereby avoiding the need of a special transition piece. By means of this intersection, the downstream ends of the shells 12a-d and the downstream ends of the premix gas channels 13a-d are bordered by cylindrical intersecting planes 16 and 17, which make it possible to slide a cylindrical burner ring 18 into the shell arrangement (FIG. 1) in order to fix the downstream ends of the shells 12a-d. The premix burner 10 with the attached burner ring 18 can Then be introduced into an essentially cylindrical coaxial burner sleeve 19 shown fig 2 ,

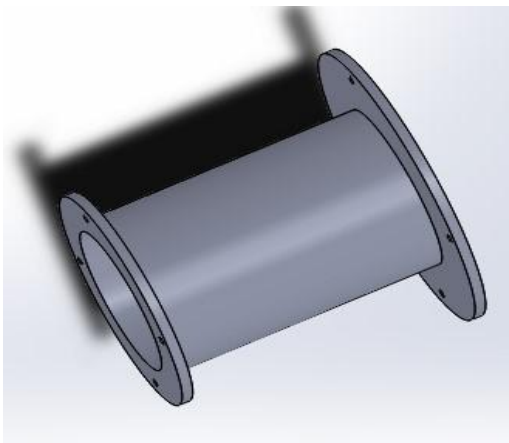


Figure 2: Sketch sleeve of burner (part no 19)

The EV-10 4 cutters shown in Fig. 1 consists of four shifted quarter cones the diameter of Each cone- quarter at the outlet is $D = 82$ mm. This diameter is used as a reference length for all Characteristic numbers with four slots between each cones, such that air is forced to enter into the cone circumferentially. The resulting swirling airflow generates recirculation zone along the centerline at the EV-10 outlet. The main fuel is injected through 124 boreholes, 0.8 mm diameter each, that are distributed equidistantly along the four air slots between the apex and the burner exit. The main fuel is mixed with the swirling air resulting in a nearly premixed combustion, EV-10 burner with an outlet outer diameter of nearly 100 mm that was used in this study the special design of the EV-burner guarantees flame stabilization at the burner exit.

The Pilot Injector

The pilot injector is mounted on the centerline inner the burner, upstream of the internal recirculation zone. The arts of injection (fuel only, air and fuel premixed, and air only) as well as the shape and axial location of the injector are exhaustively investigated at different overall equivalence

ratios.

Two different pilot injectors are used: a single injection pilot and a multi injection pilot. See fig 3 The single injection pilot contains a single hole with diameter of 5mm. The multi injection pilot has 5 holes of 1 mm orifice diameter one at the center and 4 holes of 45° around it. Three pilot locations inside the burner are tested ($X_p/X_{max} = 0, 0.5, \text{ and } 0.68$). Forcing the flame to stabilize outside the burner should be regarding NOx emission positive, as it ensures a long enough mixing path of gas and air, and would also prevent the oscillating movement of the flame which could lead to strong instabilities. To achieve this, a new pilot injector is designed where a high amount of air is injected through a reduced number of holes. The strong jet momentum thus achieved, has a strong impact on the flow field and should make possible to force the flame to stabilize outside of the burner, preventing instabilities and ensuring low NOx emissions. Different pilot injectors are tested and the multi injection pilot showed good results in stability without NOx penalties (Emara 2009).

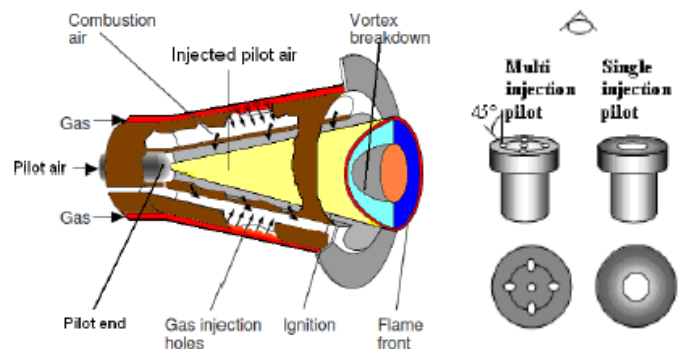


Figure 3: Sketch of the Swirl Stabilized Burner (left) and the Pilot Injectors (right).

The tested burner as shown in (Fig4) consists of an air jet surrounded by a fuel jet which is also surrounded by an outer air jet. The burner is made of two cast iron pipes as detailed on the figure.

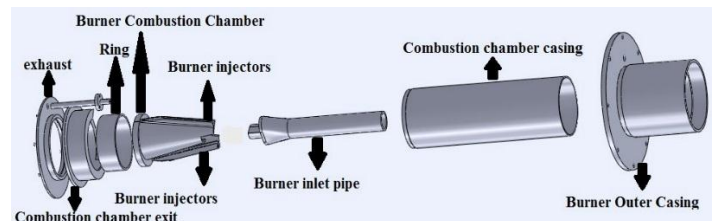


Figure4: Assembly of EV burner components

Combustor (Fig5)

The combustor is a vertically cylindrical air-cooled flame tube of 230 mm inside diameter and 300 mm long with 18 bore holes 8 mm diameter to access probe of Thermocouple to measure in flame temperature. During the combustion process, these openings are closed with 8 mm screws of



stainless steel 316. The Combustor Manufactured of thick steel pipe of 5 mm thickness. a water-cooled resonance tube of the same diameter and 1050 mm in length is attached to this combustion chamber with one bore hole 8 mm diameter

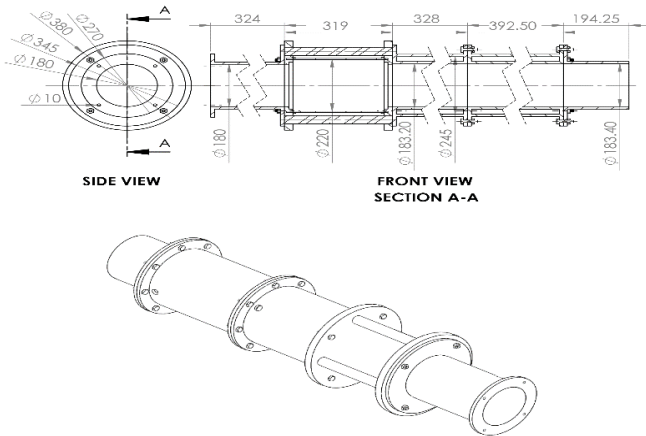


Figure 5: Combustor

Acoustic measuring system:

Microphone setup

A condenser microphone is used to measure the acoustics oscillations downstream flow. It is mounted at the position which is able to record clearly these oscillations. The used microphone is GRAS- type 26AC- S7. It is a ¼" preamplifier with a 3-m lightweight cable terminating in a 7-pin LEMO series 1B plug and used for high-frequency measurements and high-pressure measurements with wide frequency range, low noise level and very small size. The cable is only 2.5 mm in diameter and withstands temperatures from -40°C to +150°C. The typical capacitance of ¼" microphone capsule is 6.5 pF. The electrical circuit in this type of microphones is built on a ceramic substrate using selected low-noise components to gain very low self-noise. The electrical self-noise is very low that system noise is mainly determined by the microphone capsule's thermal noise. The dimensions of the microphone are as follows: 6.35mm diameter and 48mm length while the microphone weight is 4g in addition to 46g for cable and plug. As the size of the microphone is decreased, the useful frequency range of the microphone is increased. The frequency range, which can be obtained, is determined in part by the size of the microphone. The frequency range (± 0.2 dB) is 2Hz- 200 kHz. It has a flat pressure frequency response in its entire frequency range. The frequency response of the microphone is determined by the diaphragm tension, the diaphragm mass, and the acoustical damping in the airgap between the diaphragm and the back plate see Fig.6. When the sound pressure in the sound field fluctuates, the distances between the diaphragm and the back plate will change, and consequently change the capacitance of the diaphragm/back plate capacitor. As the charge on the capacitor is kept constant, the change in capacitance will generate an output voltage on the output terminal of the microphone. The acoustical performance of a microphone is determined by the physical dimensions such as diaphragm area, the distance between the diaphragm and the

back plate, the stiffness and mass of the suspended diaphragm, and the internal volume of the microphone casing.

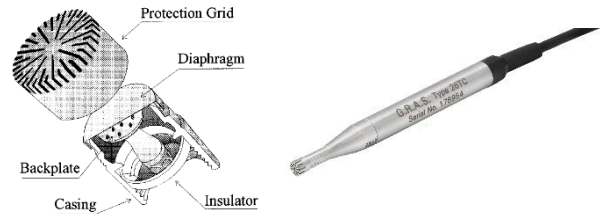


Figure 6: Basic elements of a condenser microphone

It is calibrated by using a Brüel& Kjaer pistonphone type-4228 at reference frequency 250 Hz and nominal gain of 124dB and the sensitivity was 1.152mV/pa. This type of microphones has proven to be superior with respect to temperature stability, long-term stability, and insensitivity to rough handling. It is designed and produced to ensure well-defined and accurate measurements. The operating temperature is in range of -20°C- +60°C at relative humidity of 0- 90%. The diaphragm and the back plate form the parallel plates of an air capacitor. This capacitor is polarized with a charge from an external voltage supply (externally polarized type) or by an electric charge injected directly into an insulating material on the back plate (pre-polarized type). The supply can vary between 28 VDC and 120 VDC single-sided or ± 14 VDC and ± 60 VDC dual sided.

Signal record:

The output signal from the condenser microphone measured and recorded using Agilent 3000 Series oscilloscope (Fig.7) with up to 1 GSa/s sample rate, Up to 4 kpts memory, Automatic voltage and time measurements (20) and cursor measurements, Advanced triggering (edge, pulse width, and video). Math function waveforms: add, subtract, multiply, FFT, USB ports (1 host with rear panel module, 1 device) for easy printing, saving, and sharing of waveforms, setups, screen BMP files, and CSV data files, Internal storage for 10 waveforms and 10 setups. Special digital filter and waveform recorder. Built- in 5- digit hardware frequency counter. The oscilloscope's sampling and acquisition modes according to The Nyquist sampling theorem states that for a limited bandwidth (band- limited) signal with maximum frequency f_{MAX} , the equally spaced sampling frequency f_s must be greater than twice the maximum frequency f_{MAX} , in order to have the signal be uniquely reconstructed without aliasing.

$$f_{MAX} = f_s/2 = \text{Nyquist frequency } (f_N) = \text{folding frequency}$$

Aliasing occurs when signals are under- sampled ($f_s < 2f_{MAX}$). Aliasing is the signal distortion caused by low frequencies falsely reconstructed from an insufficient number of sample points.



Figure 7: Agilent 3000 Series oscilloscope

The oscilloscope can operate in normal, average, or peak detect acquisition modes.

The trigger determines when captured data should be stored and displayed. When a trigger is set up properly, it can convert unstable displays or blank screens into meaningful waveforms. When the oscilloscope starts to acquire a waveform, it collects enough data so that it can draw the waveform to the left of the trigger point. The oscilloscope continues to acquire data while waiting for the trigger condition to occur. After it detects a trigger, the oscilloscope continues to acquire enough data so that it can draw the waveform to the right of the trigger point

Experimental Program

The interpretation of the experimental data integrates between the results being obtained at two stages to form a full picture of the variations in the acoustic signature of the 4 slot Ev burners associated with the changes of the fuel equivalency ratio, with pilot fuel shift and flow conditions. Particular emphasis is given to the variations in the acoustic oscillations in different conditions.

Table (1) Experimental Program

4 slot EV burner	$V_{air} = 873 \text{ l/min}$	$\Phi = 1$	Fuel shift 3.5 %	Fuel shift 7 %	Fuel shift 14 %
			$\Phi = 0.87$	Fuel shift 3.5 %	Fuel shift 7 %

		$\Phi = 0.75$	Fuel shift 3.5 %	Fuel shift 7 %	Fuel shift 14 %
--	--	---------------	------------------	----------------	-----------------

Before conducting any experiment, the following steps are followed:

- 1- The experimental setup is checked for leaks to ensure not only a safe working environment but also to satisfy accurate measurements of the flow rates through the different gas supply passages.
- 2- The burner is aligned in the vertical position.

RESULTS and discussion

- The acoustic signature of effect fuel shift of overall equivalence ratio ($\Phi = 1$) 4-slot EV burner

Studying the frequency domain of the liberated noise coming out from the burners 4 slots noticed the principal 13 spectral lines as shown in Fig 8 (1200 Hz ,2062 Hz, 2120 Hz ,2887 Hz , 3310 Hz,3350 Hz ,4300 Hz , 4900 Hz , 5360 Hz , 6200 Hz , 6600 Hz , 8092 Hz , 9495 Hz)

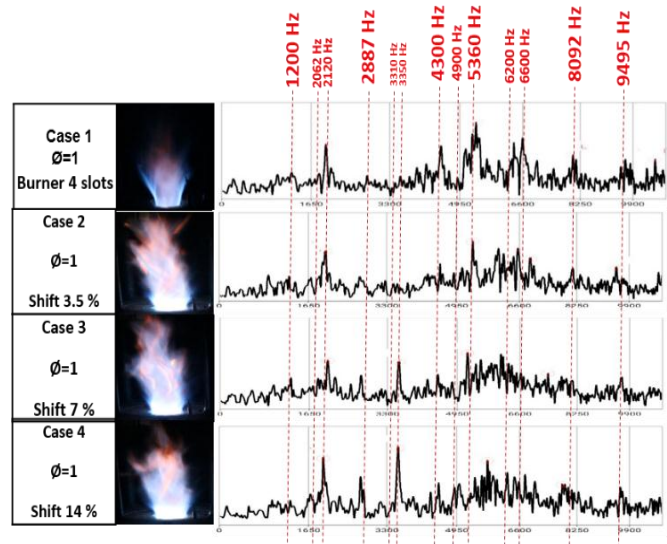


Fig 8: Acoustic signature of 4-slot burner effect fuel shift of ($\Phi = 1$)

Studying the effect of changing of fuel shift of equivalency ratio ($\Phi = 1$) at different operating condition of 4-slots burner, deduced that:

- 1- At acoustic value (1200 Hz) the highest acoustic beak formed at case 3 and the lower at case 2.
- 2- At acoustic value (2062 Hz) the highest acoustic beak formed at case 1 and the lower at case 2.
- 3- At acoustic value (2120 Hz) the highest acoustic beak formed at case 4 and the lower at case 3.



- 4- At acoustic value (2887 Hz) the highest acoustic beak formed at case 4 and the lower at case 3.
- 5- At acoustic value (3310 Hz) the highest acoustic beak formed at case 4 and the lower at case 2.
- 6- At acoustic value (3350 Hz) the highest acoustic beak formed at case 4 and the lower at case 2.
- 7- At acoustic value (4300 Hz) the highest acoustic beak formed at case 1 and the lower at case 4.
- 8- At acoustic value (4900 Hz) the highest acoustic beak formed at case 4 and the lower at case 3.
- 9- At acoustic value (5360 Hz) the highest acoustic beak formed at case 1 and the lower at case 4.
- 10-At acoustic value (6200 Hz) the highest acoustic beak formed at case 4 and the lower at case 1.
- 11-At acoustic value (6600 Hz) the highest acoustic beak formed at case 1 and the lower at case 2.
- 12-At acoustic value (8092 Hz) the highest acoustic beak formed at case 1 and the lower at case 3.
- 13-At acoustic value (9495 Hz) the highest acoustic beak formed at case 1 and the lower at case 2.

From studding the acoustic signature of the 4-slot EV burner and according to the above values the highest noise occurs at case (1).

The minor noise operating condition for the 4-slot burner is at case (2).

- The acoustic signature of effect fuel shift of overall equivalence ratio ($\Phi = 0.87$) 4-slot EV burner

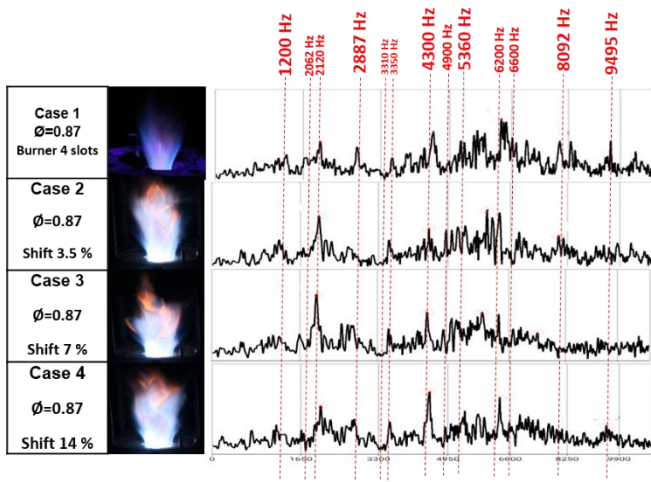


Fig 9: Acoustic signature of 4-slot burner effect fuel shift of ($\Phi = 0.87$)

Studying the frequency domain of the liberated noise coming out from the burners 4 slots noticed the principal 13 spectral lines as shown in Fig 9 (1200 Hz ,2062 Hz, 2120 Hz ,2887 Hz , 3310 Hz,3350 Hz ,4300 Hz , 4900 Hz , 5360 Hz , 6200 Hz , 6600 Hz , 8092 Hz , 9495 Hz

the effect of changing of fuel shift of equivalency ratio ($\Phi = 0.87$) at different operating condition of 4-slots burner, deduced that:

- 1- At acoustic value (1200 Hz) the highest acoustic beak formed at case 1 and the lower at case 4.
- 2- At acoustic value (2062 Hz) the highest acoustic beak formed at case 3 and the lower at case 4.
- 3- At acoustic value (2120 Hz) the highest acoustic beak formed at case 3 and the lower at case 4.
- 4- At acoustic value (2887 Hz) the highest acoustic beak formed at case 1 and the lower at case 2.
- 5- At acoustic value (3310 Hz) low acoustic beak
- 6- At acoustic value (3350 Hz) the highest acoustic beak formed at case 1 and the lower at case 3.
- 7- At acoustic value (4300 Hz) the highest acoustic beak formed at case 2 and the lower at case 4.
- 8- At acoustic value (4900 Hz) the highest acoustic beak formed at case 1 and the lower at case 2.
- 9- At acoustic value (5360 Hz) the highest acoustic beak formed at case 1 and the lower at case 2.
- 10-At acoustic value (6200 Hz) the highest acoustic beak formed at case 2 and the lower at case 3.
- 11-At acoustic value (6600 Hz) the highest acoustic beak formed at case 1 and the lower at case 2.
- 12-At acoustic value (8092 Hz) the highest acoustic beak formed at case 1 and the lower at case 3.
- 13-At acoustic value (9495 Hz) the highest acoustic beak formed at case 1 and the lower at case 3.

From studding the acoustic signature of the 4-slot EV burner and according to the above values the highest noise occurs at case (2).

The minor noise operating condition for the 4-slot burner is at case (1).

- The acoustic signature of effect fuel shift of overall equivalence ratio ($\Phi = 0.75$) 4-slot EV burner

Studying the frequency domain of the liberated noise coming out from the burners 4 slots noticed the principal 13 spectral lines as shown in Fig 10 (1200 Hz ,2062 Hz, 2120 Hz ,2887 Hz , 3310 Hz,3350 Hz ,4300 Hz , 4900 Hz , 5360 Hz , 6200 Hz , 6600 Hz , 8092 Hz , 9495 Hz)

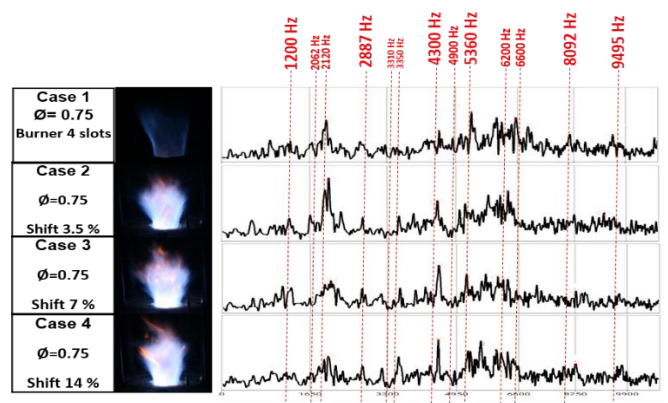


Fig 10: Acoustic signature of 4-slot burner effect fuel shift of ($\Phi = 0.75$)



Studying the effect of changing of fuel shift of equivalency ratio ($\Phi = 0.75$) at different operating condition of 4-slots burner, deduced that:

- 1- At acoustic value (1200 Hz) the highest acoustic beak formed at case 3 and the lower at case 4.
- 2- At acoustic value (2062 Hz) the highest acoustic beak formed at case 2 and the lower at case 3.
- 3- At acoustic value (2120 Hz) the highest acoustic beak formed at case 2 and the lower at case 4.
- 4- At acoustic value (2887 Hz) the highest acoustic beak formed at case 3 and the lower at case 1.
- 5- At acoustic value (3310 Hz) low acoustic beak.
- 6- At acoustic value (3350 Hz) the highest acoustic beak formed at case 4 and the lower at case 1.
- 7- At acoustic value (4300 Hz) the highest acoustic beak formed at case 3 and the lower at case 1.
- 8- At acoustic value (4900 Hz) low acoustic beak.
- 9- At acoustic value (5360 Hz) the highest acoustic beak formed at case 1 and the lower at case 2.
- 10-At acoustic value (6200 Hz) the highest acoustic beak formed at case 4 and the lower at case 1.
- 11-At acoustic value (6600 Hz) the highest acoustic beak formed at case 1 and the lower at case 2.
- 12-At acoustic value (8092 Hz) the highest acoustic beak formed at case 1 and the lower at case 3.
- 13-At acoustic value (9495 Hz) the highest acoustic beak formed at case 2 and the lower at case 3.

From studding the acoustic signature of the 4-slot EV burner and according to the above values the highest noise occurs at case (1).

The minor noise operating condition for the 4-slot burner is at case (3).

REFERENCES

- [1] Yang, V., and Lieuwen, T. C., "Combustion Instabilities in gas turbine engines: Operational experience, fundamental Mechanisms, and Modeling", Vol.210 Progress in Astronautics and Aeronautics, Arlington, Texas, 2005.
- [2] Emara, A., Lacarelle, A., Paschereit, C. O., "Pilot Flame Impact on Flow Fields and Combustion Performances in a Swirl inducing Burner", AIAA 2009-5015, August 2009, Denver, Colorado, USA.
- [3] Rankin, D.D., "Lean Combustion", Elsevier Inc., 2007.
- [4] Seyfried, H., Brackmann, C., Lindholm, A., Linne, M., Aldén, M., Barreras, F., and Bank, R., "Optical Investigations of the Combustion Characteristics of a Gas Turbine Pilot Burner", 45th AIAA Aerospace Sciences Meeting and Exhibit 8 - 11 January 2007, Reno, Nevada.

[5] Giampaolo, T., "The Gas Turbine Handbook: Principles and Practices", 2nd Edition, the Fairmont Press, 2003.

[6] Albrecht, P., Bade, S., Paschereit, C.O., Gutmark, E., "Avoidance strategy for NOx emissions and flame instabilities in a swirl-stabilized combustor", AIAA20091059 paper, 2008.

[7] Lacarelle, A.; Luchtenburg, D. M.; Bothien, M. R.; Noack, B. R. & Paschereit, C. O. "Coherent Structure Characterization of Premixed Flames under Varying Forcing Conditions" Int. Conf. on Jets, Wakes and Separated Flows, September 16 – 19, 2008, Berlin, Germany, 2008.

[8] Paschereit, C. O., Gutmark, E. J., Weisenstein, W., 1999, "Coherent structures in swirling flows and their role in acoustic combustion control", Physics of Fluids, vol. 11, pp. 2667-2678.

[9] Sameh Hassan, Ahmed Emara, Mahmoud Elkady "Evaluation of EV Burner Performance through Pilot Injection Technology: A Review" 2016